

# Morphology of Inflationary Gravitational Wave Spectra imprinted by a Sequence of Post-Inflationary Epochs via GWInSpect

Swagat S. Mishra <sup>a,b</sup> Athul K. Soman  <sup>c</sup>

<sup>a</sup>School of Physics and Astronomy, University of Nottingham, Nottingham, NG7 2RD, UK.

<sup>b</sup>Cosmology, Gravity, and Astroparticle Physics Group, Center for Theoretical Physics of the Universe (CTPU-CGA), Institute for Basic Science (IBS), Daejeon, 34126, Korea.

<sup>c</sup>International School for Advanced Studies (SISSA), via Bonomea 265, 34136 Trieste, Italy.

E-mail: [swagat.mishra@nottingham.ac.uk](mailto:swagat.mishra@nottingham.ac.uk), [akuruvai@sissa.it](mailto:akuruvai@sissa.it)

**Abstract.** Expansion history of the Universe, prior to the onset of Big Bang Nucleosynthesis (BBN), remains largely unknown. The high-energy post-inflationary era is, in general, expected to be complex, potentially consisting of multiple distinct epochs, each characterized by a distinct equation of state (EoS). One of the robust predictions of the inflationary paradigm is the generation of tensor perturbations through quantum fluctuations, which later manifest as a stochastic background of primordial gravitational waves (GWs). The large-scale amplitude and small-scale spectral tilt ( $n_{\text{GW}}$ ) of inflationary GWs encode information about the energy scale of inflation, and provide an important observational probe of the post-inflationary (pre-BBN) dynamics, respectively. In particular, a softer post-inflationary EoS ( $w < 1/3$ ) leads to red-tilted GW spectrum ( $n_{\text{GW}} < 0$ ), whereas stiffer EoS ( $w > 1/3$ ) produces blue tilt ( $n_{\text{GW}} > 0$ ).

In the previous work [1], we developed an analytical framework for computing the spectral energy density of these first-order GWs for scenarios involving multiple sharp (instantaneous) transitions in the post-inflationary EoS,  $w_1 \rightarrow w_2 \rightarrow \dots \rightarrow w_n \rightarrow w_{n+1} = 1/3$ . We primarily focused on determining the parameter space which leads to GW signals that may be detectable by future GW observatories.

In this companion paper, we extend the framework of Ref. [1] to systematically explore the rich landscape of possible inflationary GW spectra imprinted by multiple ( $n \gg 1$ ) post-inflationary epochs prior to the hot Big Bang. Remaining agnostic to specific models, we demonstrate that a *diverse morphological zoo of spectral shapes*—ranging from convex and concave monotonic profiles to highly non-monotonic features—can emerge depending on the sequence and duration of epochs. We introduce **GWInSpect** —a Python-based, user-friendly package that efficiently generates inflationary GW spectra for arbitrary post-inflationary histories, enabling a systematic study of the post-inflationary expansion history.

**Keywords:** Inflation, Gravitational Waves

**ArXiv ePrint:** [arXiv:2510.25672](https://arxiv.org/abs/2510.25672)

---

## Contents

<b>1</b>	<b>Introduction</b>	<b>1</b>
<b>2</b>	<b>Inflationary gravitational waves</b>	<b>3</b>
2.1	Evolution of tensor mode functions through multiple post-inflationary epochs	4
2.2	Spectral energy density and present-epoch frequency of inflationary GWs	6
2.3	Analytical treatment of the BBN bound on stochastic GWs	7
<b>3</b>	<b>The morphological zoo of inflationary gravitational wave spectra</b>	<b>8</b>
3.1	Scenarios with monotonic spectra of inflationary gravitational waves	10
3.1.1	Blue-tilted inflationary GWs with convex-shaped spectra	11
3.1.2	Blue-tilted inflationary GWs with concave-shaped spectra	12
3.2	Scenarios with non-monotonic spectra of inflationary gravitational waves	12
3.2.1	Non-monotonic spectra for a soft EoS immediately after inflation	12
3.2.2	Non-monotonic spectra for a stiff EoS immediately after inflation	13
<b>4</b>	<b>GWInSpect: Python-based numerical package</b>	<b>14</b>
4.1	Overview	14
4.2	Required inputs	15
4.3	Typical outputs	16
<b>5</b>	<b>Discussion and Outlook</b>	<b>16</b>
<b>6</b>	<b>Acknowledgements</b>	<b>17</b>

---

## 1 Introduction

Cosmic inflation [2–15] is the leading paradigm for providing initial conditions for the hot Big Bang phase [7, 16–18]. In its simplest realization, inflation is driven by a scalar field  $\phi$ , the *inflaton*, which is minimally coupled to gravity, and slowly rolls down its potential  $V(\phi)$  [7, 9, 10, 15]. Quantum fluctuations of the inflaton field give rise to a nearly scale-invariant spectrum of scalar perturbations [19–22], whose imprints on the Cosmic Microwave Background (CMB) [23–26] and the large-scale structure [17, 27, 28] strongly support the single-field slow-roll inflationary framework.

Alongside scalar perturbations, inflation also generates tensor quantum fluctuations, which constitute a stochastic background of primordial gravitational waves (GWs) [29–32]. Their spectral energy density ( $\Omega_{\text{GW}}$ ) on large cosmological scales contains information about the energy scale of inflation [1, 30, 31, 33–35], while its spectral tilt ( $n_{\text{GW}}$ ), particularly on small scales, is sensitive to the post-inflationary equation of state (EoS),  $w$ , of the early Universe [1, 31]. To be precise, a softer EoS, with  $w < 1/3$ , results in a red tilt, while a stiffer EoS, with  $w > 1/3$ , leads to blue-tilted GWs, which are of great phenomenological interest from an observational prospect. Consequently, the inflationary GW spectrum offers a unique window into the expansion history of the Universe between the end of inflation and the onset of Big Bang Nucleosynthesis (BBN) – which remains observationally unconstrained at present [1, 15, 36–39].

A broad network of GW detectors, operating across frequencies from  $10^{-18}$  Hz to  $10^3$  Hz, is now capable of probing this primordial signal. These include CMB B-mode experiments such as BICEP/Keck [40], LiteBIRD [41], and the Simons Observatory [42]; pulsar timing arrays (PTAs) such as NANOGrav [43, 44], EPTA/InPTA [45, 46], and IPTA [47]; and laser interferometers such as LIGO/Virgo/KAGRA [48–50] and future missions including LISA [51], DECIGO [52], BBO [53], Cosmic

**Explorer** [54], and the **Einstein Telescope** [55]. These facilities together span a significant frequency range of inflationary tensor modes.

The post-inflationary Universe is expected to have undergone a complex sequence of phases and non-equilibrium processes before reaching the radiation-dominated phase [56–59] prior to the commencement of BBN. The dynamics of reheating and subsequent transitions can, therefore, involve several distinct epochs [35, 60–65], each characterized by a different effective EoS,  $w_i$ . Most works in the literature have typically assumed a single average EoS during reheating [66–70]. In our previous work [1], we developed an analytical framework based on Israel junction-matching conditions [31, 71, 72] to compute the spectrum of the first-order inflationary GWs for multiple ( $n$ -number of) sharp (instantaneous) transitions in the post-inflationary EoS,  $w_1 \rightarrow w_2 \rightarrow \dots \rightarrow w_n \rightarrow 1/3$ . We primarily focused on identifying the parameter space of post-inflationary EoS and transition energy scales,  $\{w_i, E_i\}$ , that leads to the spectra of inflationary GWs which are consistent with the existing constraints from **aLIGO** and BBN, while being potentially detectable by future observatories. In fact, Ref. [1] dealt with up to 4 different post-inflationary epochs before the hot Big Bang.

In this companion paper, we utilise the framework developed in Ref. [1] to systematically characterise the *morphological zoo of inflationary GW spectra* emerging from a large number of sequential post-inflationary epochs ( $n \approx 10$ ). We remain agnostic about the specific model details, and allow the EoS of any epoch to lie in the range  $w_i \in (-1/3, 1)$ . We demonstrate that a remarkably diverse range of spectral shapes – convex, concave, monotonic, and non-monotonic – can arise purely from the sequence and duration of these epochs. We further develop a simple and user-friendly Python-based *numerical package*, called **GWInSpect** (GitHub link [🔗](#)) that facilitates the interested users to generate such spectra for arbitrary post-inflationary histories within this general framework. In fact, one of the key objectives of this work is to highlight the efficiency of **GWInSpect** package. With a simple interface and fast performance, it enables the exploration of complex sequences of epochs with minimal effort, making it ideal for large parameter scans or integration into broader cosmological analyses. We provide an instructive tutorial with an `ipynb` notebook in the same GitHub page, which can be directly accessed from the link: [tutorial notebook](#). By providing this package publicly, we positively aim to encourage its widespread use for systematically investigating the imprints of diverse post-inflationary scenarios on the gravitational wave background.

To be precise, the present paper differs from our previous work in Ref. [1] in the following distinct ways:

- The previous work in Ref. [1] presented a comprehensive analytical and numerical framework for computing the spectral energy density of inflationary GWs, corresponding to multiple post-inflationary epochs in the early Universe. The primary goal was to determine the viable parameter space of the post-inflationary Universe – in particular, the equation-of-state parameters and the energy scales of successive transition epochs – that could yield an observable GW signal in upcoming and future detectors, while remaining consistent with existing constraints from BBN and **aLIGO**.

In the present work, we instead utilise the analytical formalism developed in Ref. [1] to systematically categorise the wide variety of inflationary GW spectra that can emerge from multiple EoS transitions. While all our results respect the BBN constraints, we do not focus here on detectability forecasts or comparison with experimental sensitivities. In contrast, the present paper adopts a narrower focus, emphasizing the diversity of possible spectral shapes arising from multiple post-inflationary epochs. Since our analytical approach relies on the instantaneous transition approximation between successive epochs, each post-inflationary phase is required to last at least one  $e$ -fold for a reliable estimate of the GW spectrum.

- Ref. [1] applied the formalism to model-agnostic post-inflationary histories, as well as to a specific string theory inspired scenario. The current work, on the other hand, is fully model-independent and aims to illustrate the generic features of the inflationary GW spectrum without reference to any particular particle-physics model.
- Building upon the numerical infrastructure developed previously, we introduce a dedicated publicly available numerical package, **GWInSpect**, which efficiently computes the inflationary GW spectrum for arbitrary sequences of post-inflationary epochs characterized by multiple EoS parameters  $\{w_i\}$ . The code allows the user to generate spectra across a wide frequency range within a short runtime.

The paper is organized as follows. In Sec. 2, we summarize the relevant analytical expressions for the tensor mode functions in the post-inflationary epochs, and the corresponding GW spectral energy density, using the junction matching formalism discussed in Ref. [1]. In Sec. 3, we present the wide variety of possible spectral shapes of inflationary GWs corresponding to different post-inflationary expansion histories. Sec. 4 describes our lightweight Python-based numerical package, **GWInSpect**, for computing these spectra efficiently. Finally, Sec. 5 summarizes our main conclusions and provides further discussion.

### Units, Notation & Convention

- We mostly work in natural units, where  $\hbar, c = 1$ .
- The reduced Planck mass is defined to be  $m_p = \frac{1}{\sqrt{8\pi G}} = 2.44 \times 10^{18} \text{ GeV}$ .
- The background universe is considered to be described by the flat Friedmann-Lemaître-Robertson-Walker (FLRW) line element, with scale factor  $a(t)$  and Hubble parameter  $H(t)$ .
- Conformal time ( $\tau$ ) is related to the cosmic time ( $t$ ) by  $d\tau = \frac{dt}{a(t)}$ .
- Fourier mode functions  $h_k(\tau)$  of a field  $h(\tau, \vec{x})$  are defined as

$$h(\tau, \vec{x}) = \int \frac{d^3 \vec{k}}{(2\pi)^3} h_k(\tau) e^{i \vec{k} \cdot \vec{x}}.$$

- Derivative of the mode functions *w.r.t* cosmic time  $t$  is denoted as an *overdot*,  $\frac{dh_k}{dt} \equiv \dot{h}_k$  and *w.r.t* conformal time  $\tau$  is denoted as an *overprime*,  $\frac{dh_k}{d\tau} \equiv h'_k$ .
- The dimensionless Hubble constant, denoted as  $h$ , is defined by  $h = H_0 / [100 \text{ (km/sec/Mpc)}]$  [not to be confused with the tensor field  $h(\tau, \vec{x})$ , or the tensor mode functions  $h_k(\tau)$ ].

To remain consistent, we follow the same notation and convention as used in Ref. [1].

## 2 Inflationary gravitational waves

The accelerated expansion of space during inflation leads to the amplification of vacuum tensor fluctuations [29], which are stretched to super-Hubble scales [30], where they remain effectively frozen until their subsequent Hubble re-entry in the post-inflationary (decelerating) Universe. Once these tensor modes re-enter the Hubble radius, they begin to oscillate and propagate as primordial GWs. Modes with higher frequencies (shorter wavelengths) re-enter the Hubble radius at earlier times after inflation, whereas modes with lower frequencies (longer wavelengths) re-enter at later epochs. Having been generated during inflation, the tensor modes propagate largely unimpeded

to the present epoch, thereby retaining key imprints of the intermediate expansion history of the Universe. In particular, the high-frequency regime of the spectrum, corresponding to present-day frequencies  $f \gg 10^{-10}$  Hz, encodes valuable information about the unknown pre-BBN evolution of the Universe (see Sec. 2.2), as discussed in Refs. [1, 31, 67]. In what follows, we summarise the essential analytical framework required for computing the spectral energy density of inflationary GWs, restricting ourselves to those expressions most relevant for the present study. A detailed treatment of the same can be found in our previous work [1].

## 2.1 Evolution of tensor mode functions through multiple post-inflationary epochs

Evolution of the Fourier mode functions of primordial tensor fluctuations generated by inflation, at linear order in perturbation theory, is governed by the following second-order differential equation

$$h_k''^\lambda + 2 \left( \frac{a'}{a} \right) h_k'^\lambda + k^2 h_k^\lambda = 0, \quad (2.1)$$

where  $h_k^\lambda$  is the tensor amplitude, with  $\lambda = \{+, \times\}$  denoting the two polarisation of GWs and  $k$  is the comoving wavenumber of the tensor modes. General solution to Eq. (2.1) can be written as a linear combination of two Bessel functions of the first kind [73], namely,  $\{J_{(\alpha-\frac{1}{2})}(x), J_{-(\alpha-\frac{1}{2})}(x)\}$ , as follows—

$$h_k^\lambda(y_k) = \frac{1}{(\alpha y_k)^{\alpha-\frac{1}{2}}} \left[ A_k J_{(\alpha-\frac{1}{2})}(\alpha y_k) + B_k J_{-(\alpha-\frac{1}{2})}(\alpha y_k) \right], \quad (2.2)$$

where  $\alpha$  is related to the EoS ( $w$ ), while  $y_k(\tau)$  is the physical frequency ( $k/a(\tau)$ ) of the tensor modes—scaled by the Hubble parameter ( $H(\tau)$ ), of the post-inflationary Universe, *i.e.*,

$$\alpha = \frac{2}{1+3w}, \quad y_k(\tau) = \frac{k}{a(\tau)H(\tau)}. \quad (2.3)$$

The Bogoliubov coefficients,  $\{A_k, B_k\}$ , are determined by imposing the appropriate initial or boundary conditions on the tensor mode functions. For the first post-inflationary epoch, characterised by a constant EoS ( $w_1$ ), these coefficients are obtained by matching to the inflationary tensor modes at the end of inflation. Specifically, the super-Hubble inflationary tensor perturbations serve as the initial conditions for the subsequent evolution in this epoch. Consequently, for any mode with comoving wavenumber  $k$  that was super-Hubble at the onset of the first epoch, the initial tensor mode function is taken to be equal to the frozen amplitude of the corresponding inflationary mode, while its time derivative vanishes, namely,

$$h_k^\lambda(\tau_k) = h_{k,\text{inf}}^\lambda \quad ; \quad h_k'^\lambda(\tau_k) = 0, \quad (2.4)$$

where  $\tau_k$  marks the post-inflationary Hubble-entry time of a tensor mode of interest with (comoving) wavenumber  $k$ . Eq. (2.4) yields the following expression for the Bogoliubov coefficients for the first epoch (see Ref [1])

$$A_{k,1} = 2^{(\alpha_1-\frac{1}{2})} \Gamma \left( \alpha_1 + \frac{1}{2} \right) h_{k,\text{inf}}^\lambda, \quad B_{k,1} = 0, \quad (2.5)$$

where  $\Gamma(x)$  is the Gamma function.

As emphasized earlier, the high-energy post-inflationary dynamics of the Universe is expected to involve a variety of complex physical processes, potentially giving rise to multiple distinct expansion phases before the onset of BBN. It is therefore instructive to model the pre-BBN expansion history as a sequence of successive cosmic epochs, each characterised by a (nearly) constant EoS parameter [1, 74, 75], as illustrated in Fig. 1. We denote this sequence of post-inflationary EoS parameters by  $w_1, w_2, \dots, w_n, w_{n+1} = 1/3$ , where  $w_{n+1}$  is the EoS of the radiation-dominated hot Big Bang phase.

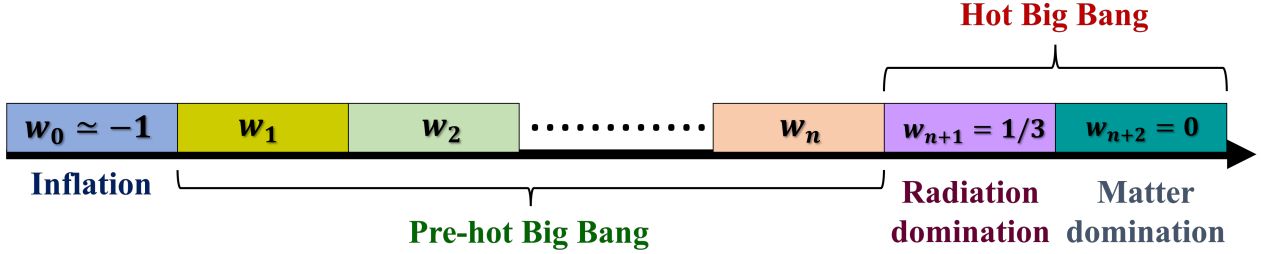


**Figure 1:** A schematic depiction of the timeline of the universe featuring multiple post-inflationary epochs, each described by a nearly constant equation of state parameter. Note that the horizontal length is not a representation of the actual duration.

In addition, by assuming that the transition between any two successive epochs is sufficiently sharp, *i.e.*, effectively instantaneous, one can employ the Israel junction conditions [71] to relate the tensor mode functions across the transition. This procedure allows the Bogoliubov coefficients, and hence the mode functions in a succeeding epoch, to be determined directly from those in the preceding epoch. The junction conditions can be expressed as follows—

$$h_{k,b}^\lambda(\tau_i) = h_{k,a}^\lambda(\tau_i), \quad [\text{Continuity}], \quad (2.6)$$

$$h'_{k,b}^\lambda(\tau) \Big|_{\tau=\tau_i} = h'_{k,a}^\lambda(\tau) \Big|_{\tau=\tau_i}, \quad [\text{Differentiability}]. \quad (2.7)$$

Here,  $h_{k,b}^\lambda$  and  $h_{k,a}^\lambda$  denote, respectively, the tensor mode functions immediately before and after a transition occurring at conformal time  $\tau = \tau_i$ . The general form of the tensor mode function in the  $i^{\text{th}}$  post-inflationary epoch (which ends at  $\tau_i$ ), characterised by its corresponding Bogoliubov coefficients  $A_{k,i}$  and  $B_{k,i}$ , can then be written as (see Ref. [1])

**Mode functions :**

$$h_{\mathbf{k}}^\lambda(y_k) = \frac{1}{(\alpha_i y_k)^{\alpha_i - \frac{1}{2}}} \left[ \mathbf{A}_{\mathbf{k},i} J_{(\alpha_i - \frac{1}{2})}(\alpha_i y_k) + \mathbf{B}_{\mathbf{k},i} J_{-(\alpha_i - \frac{1}{2})}(\alpha_i y_k) \right], \quad (2.8)$$

**Bogoliubov coefficients :**

$$\mathbf{A}_{\mathbf{k},i} = \frac{(\alpha_i y_{k,i-1})^{(\alpha_i - \frac{1}{2})}}{(\alpha_{i-1} y_{k,i-1})^{(\alpha_{i-1} - \frac{1}{2})}} \frac{[\mathbf{A}_{\mathbf{k},i-1} (g_2 f_3 + g_4 f_1) + \mathbf{B}_{\mathbf{k},i-1} (f_2 f_3 - f_4 f_1)]}{f_1 g_3 + g_1 f_3}, \quad (2.9)$$

$$\mathbf{B}_{\mathbf{k},i} = \frac{(\alpha_i y_{k,i-1})^{(\alpha_i - \frac{1}{2})}}{(\alpha_{i-1} y_{k,i-1})^{(\alpha_{i-1} - \frac{1}{2})}} \frac{[\mathbf{A}_{\mathbf{k},i-1} (g_2 g_3 - g_4 g_1) + \mathbf{B}_{\mathbf{k},i-1} (f_2 g_3 + f_4 g_1)]}{f_1 g_3 + g_1 f_3}, \quad (2.10)$$

with **dimensionless wavenumber** :

$$y_{k,i-1} = \frac{k}{a(\tau_{i-1}) H(\tau_{i-1})}, \quad (2.11)$$

and the **Bessel constants** :

$$\begin{aligned} g_1 &= J_{(\alpha_i - \frac{1}{2})}(\alpha_i y_{k,i-1}), & f_1 &= J_{-(\alpha_i - \frac{1}{2})}(\alpha_i y_{k,i-1}), \\ g_2 &= J_{(\alpha_{i-1} - \frac{1}{2})}(\alpha_{i-1} y_{k,i-1}), & f_2 &= J_{-(\alpha_{i-1} - \frac{1}{2})}(\alpha_{i-1} y_{k,i-1}), \\ g_3 &= J_{(\alpha_i + \frac{1}{2})}(\alpha_i y_{k,i-1}), & f_3 &= J_{-(\alpha_i + \frac{1}{2})}(\alpha_i y_{k,i-1}), \\ g_4 &= J_{(\alpha_{i-1} + \frac{1}{2})}(\alpha_{i-1} y_{k,i-1}), & f_4 &= J_{-(\alpha_{i-1} + \frac{1}{2})}(\alpha_{i-1} y_{k,i-1}). \end{aligned} \quad (2.12)$$

It is important to emphasize that the analytical formalism employed in this work, based on the aforementioned usage of instantaneous transitions and Israel junction matching conditions, is reliable only when each post-inflationary epoch persists for a minimum duration of at least one  $e$ -fold. This requirement ensures that the background dynamics within each constant  $w_i$  phase can be treated as quasi-stationary, thereby preserving the adiabatic evolution of tensor modes across transitions. If an epoch were to last for a substantially shorter duration, the assumption of a well-defined constant EoS would break down, and the discontinuous matching conditions would no longer provide a reliable description of the gravitational wave dynamics. In practice, this consistency condition has been incorporated within our numerical framework, **GWInSpect**, discussed in Sec. 4.

## 2.2 Spectral energy density and present-epoch frequency of inflationary GWs

The spectral energy density of the gravitational waves is a measure of the GW energy density per logarithm interval of frequency [76, 77], defined as,

$$\Omega_{\text{GW}}(\tau, k) = \frac{1}{\rho_c} \frac{d}{d \ln k} \rho_{\text{GW}}(\tau, k), \quad (2.13)$$

where  $\rho_{\text{GW}}$  is the energy density of GWs and  $\rho_c(\tau) = 3 m_p^2 H^2(\tau)$  is the critical energy density. In the sub-Hubble regime—when a tensor mode is sufficiently inside the Hubble radius—expression for the GW spectral energy density becomes [1]

$$\Omega_{\text{GW}}(\tau, k) = \frac{1}{12} \left[ \frac{k}{a(\tau) H(\tau)} \right]^2 \mathcal{P}_h(\tau, k), \quad (2.14)$$

where  $\mathcal{P}_h(\tau, k) = 2 k^3 |h_k|^2 / (2\pi^2)$  is the total tensor power spectrum (including both polarization states) at conformal time  $\tau$ . By evolving the tensor modes to the present epoch and considering the sub-Hubble regime, one can compute the tensor power spectrum today and thereby obtain the present-day spectral energy density of GWs, which, when averaged over the oscillations of individual modes, takes the following form—

$$\overline{\Omega_{\text{GW}}(\tau_0, k)} = \left( \frac{\Omega_{\text{rad},0}}{96\pi^3} \right) \left( \frac{g_{*,\text{r}*}}{g_{*,0}} \right) \left( \frac{g_{s,0}}{g_{s,\text{r}*}} \right)^{4/3} \frac{1}{y_{k,\text{eq}}^2} \left[ \tilde{A}_{k,\text{MD}}^2 + \tilde{B}_{k,\text{MD}}^2 \right] \frac{H_{\text{inf}}^2}{m_p^2} \left( \frac{k}{k_*} \right)^{n_T}. \quad (2.15)$$

Here,  $g_*$  and  $g_s$  denote, respectively, the effective number of relativistic degrees of freedom contributing to the energy and entropy densities of the Universe;  $\Omega_{\text{rad},0}$  is the present-epoch radiation density parameter,  $n_T$  represents the primordial (inflationary) tensor spectral tilt,  $k_*$  is the CMB pivot scale,  $\text{r}_*$  denotes the beginning of hot Big Bang, and finally,  $y_{k,\text{eq}} \equiv k/(a_{\text{eq}} H_{\text{eq}})$ , with the subscript “eq” referring to the epoch of matter–radiation equality. The re-scaled Bogoliubov coefficients corresponding to the standard matter-dominated epoch are defined as  $\tilde{A}_{k,\text{MD}} \equiv A_{k,\text{MD}}/h_{k,\text{inf}}^\lambda$  and  $\tilde{B}_{k,\text{MD}} \equiv B_{k,\text{MD}}/h_{k,\text{inf}}^\lambda$ .

Eq. (2.15) can be conveniently re-expressed in terms of the present-day GW frequency, which is a directly measurable quantity in GW observations. Since the primordial tensor spectral index is constrained to be very small ( $|n_T| \ll 1$ ), its effect on the overall amplitude and tilt of the spectrum is negligible compared to that arising from the post-inflationary dynamics. Therefore, we set  $n_T = 0$  throughout this analysis in order to isolate and highlight the imprints of the pre–hot Big Bang expansion history on the morphology of the GW spectral energy density. The resulting expression for the present-day spectral energy density of inflationary GWs, written as a function of the GW frequency, takes the following form [1]—

**Spectral energy density :**

$$h^2 \Omega_{\text{GW}}^{(0)}(f_k) = \frac{1}{96\pi^3} \frac{g_{*,\text{r}*}}{g_{*,0}} \left( \frac{g_{s,0}}{g_{s,\text{r}*}} \right)^{4/3} h^2 \Omega_{\text{rad},0} \left( \frac{f_{\text{eq}}}{f_k} \right)^2 \left[ \tilde{A}_{\mathbf{k},\text{MD}}^2 + \tilde{B}_{\mathbf{k},\text{MD}}^2 \right] \left( \frac{H_{\text{inf}}}{m_p} \right)^2, \quad (2.16)$$

where the **rescaled Bogoliubov coefficients** are

$$\tilde{A}_{\mathbf{k},\text{MD}} = \frac{A_{k,\text{MD}}}{h_{k,\text{inf}}^\lambda}, \quad \tilde{B}_{\mathbf{k},\text{MD}} = \frac{B_{k,\text{MD}}}{h_{k,\text{inf}}^\lambda}. \quad (2.17)$$

Relation between the present-day frequency ( $f_k$ ) of a tensor mode to the *effective* temperature ( $T_k$ ), and energy scale ( $E_k$ ), of the universe at the Hubble-entry time of that mode is given by –

**Present-day Frequency of GWs :**

$$\frac{f_k}{\text{Hz}} = 7.43 \times 10^{-8} \left( \frac{g_{s,0}}{g_{s,T_k}} \right)^{1/3} \left( \frac{g_{*,T_k}}{90} \right)^{1/2} \left( \frac{T_k}{\text{GeV}} \right) = 1.03 \times 10^{-8} \left( \frac{g_{s,0}}{g_{s,T_k}} \right)^{1/3} g_{*,T_k}^{1/4} \left( \frac{E_k}{\text{GeV}} \right). \quad (2.18)$$

The spectral tilt of  $\Omega_{\text{GW}}^{(0)}(f)$  for the range of modes making an Hubble-entry during the  $i^{\text{th}}$  post-inflationary epoch depends on the EoS of the epoch in the following way –

**Spectral tilt of GWs :**

$$n_{\text{GW}}^{(i)} \equiv \frac{d \ln \Omega_{\text{GW}}^{(0)}(f_k)}{d \ln f_k} = 2 \left( \frac{w_i - 1/3}{w_i + 1/3} \right), \quad \text{for } f_{\{i\}} < f_k < f_{\{i-1\}}. \quad (2.19)$$

### 2.3 Analytical treatment of the BBN bound on stochastic GWs

Observations of the primordial light-element abundances from BBN impose a stringent upper bound on the total energy density of primordial GWs, given by

$$h^2 \int_{f_{\text{BBN}}}^{f_{\text{end}}} d \ln f \Omega_{\text{GW}}(\tau_0, f) < 1.13 \times 10^{-6}, \quad (2.20)$$

where the integration extends from the frequency  $f_{\text{BBN}}$  corresponding to the tensor mode that re-entered the Hubble radius at the onset of BBN, up to  $f_{\text{end}}$  associated with the mode that re-entered at the end of inflation. In practice, since within any given  $i^{\text{th}}$  post-inflationary epoch the GW spectral energy density scales as  $\Omega_{\text{GW}} \propto f^{n_{\text{GW}}^{(i)}}$  (with  $n_{\text{GW}}^{(i)}$  defined in Eq. (2.19)), the BBN integral in Eq. (2.20) can be evaluated efficiently by performing a piecewise analytical integration across the different epochs, as derived in Ref. [1]. This leads to the following compact condition ensuring consistency with the BBN bound –

**BBN Constraint :**

$$\left[ \ln \left( \frac{f_{\text{r}*}}{f_{\text{BBN}}} \right) + \frac{\mathcal{F}_n}{2(1-\alpha_n)} \left\{ \left( \frac{f_{n-1}}{f_n} \right)^{2(1-\alpha_n)} - 1 \right\} + \frac{\mathcal{F}_{n-1}}{2(1-\alpha_{n-1})} \left\{ \left( \frac{f_{n-2}}{f_{n-1}} \right)^{2(1-\alpha_{n-1})} - 1 \right\} \right. \\ \left. + \dots + \frac{\mathcal{F}_1}{2(1-\alpha_1)} \left\{ \left( \frac{f_{\text{end}}}{f_1} \right)^{2(1-\alpha_1)} - 1 \right\} \right] < 1.13 \times 10^{-6} \times \left( h^2 \Omega_{\text{GW}}^{0,\text{RD}} \right)^{-1}, \quad (2.21)$$

where each  $f_i$  corresponds to the frequency of a tensor mode that re-entered the Hubble radius at the end of  $i^{\text{th}}$  epoch and while  $\mathcal{F}_i$  is defined as

$$\mathcal{F}_i = \prod_{m=i}^n \left( \frac{f_m}{f_{m+1}} \right)^{2(1-\alpha_{m+1})}, \quad \text{and} \quad i \in \{1, 2, \dots, n\}, \quad (2.22)$$

and

$$\Omega_{\text{GW}}^{0, \text{RD}} \simeq \frac{1}{24} \Omega_{\text{rad}, 0} \times \frac{2}{\pi^2} \times \left( \frac{H_{\text{inf}}}{m_p} \right)^2. \quad (2.23)$$

### 3 The morphological zoo of inflationary gravitational wave spectra

In this section, we undertake a detailed investigation into the diverse shapes that the inflationary GW spectrum can exhibit as a consequence of different post-inflationary (pre-BBN) expansion histories of the Universe. As emphasised above, the evolution of tensor modes across successive epochs, each characterized by a distinct EoS parameter  $w_i$ , imprints a rich structure on the spectral energy density  $\Omega_{\text{GW}}^{(0)}(f)$ . Depending on the sequence, duration, and relative energy scales of these epochs, the resulting spectra can display a wide range of morphologies—including monotonic (blue- or red-tilted), convex, concave, as well as non-monotonic or multi-peaked behaviours.

Our goal here is to systematically map this *zoo of inflationary GW spectra* in a model-agnostic manner, relying solely on the macroscopic post-inflationary dynamics encapsulated by the EoS parameters  $\{w_i\}$  and the transition scales  $\{E_i\}$ . By varying these parameters within the framework established in Sec. 2, we illustrate how even simple sequences of instantaneous transitions can give rise to remarkably distinct spectral features. Such an analysis not only highlights the sensitivity of  $\Omega_{\text{GW}}^{(0)}(f)$  to the early expansion history, but also provides valuable intuition for interpreting future detections of a stochastic GW background in terms of the underlying kinematics of cosmic evolution.

To be precise, different shapes of the GW spectra correspond to the following sequence of the post-inflationary expansion history—

1. The spectrum is monotonic when either  $w_i > 1/3$  (blue-tilted) or  $w_i < 1/3$  (red-tilted) for all pre-hot Big Bang epochs  $i$ .
2. A monotonic spectrum is convex when  $w_1 > w_2 > w_3 \dots > w_n$ , while it is concave when  $w_1 < w_2 < w_3 \dots < w_n$ . In the absence of a strict ordering among the EoS parameters, the resulting monotonic spectrum ceases to exhibit a definite curvature and becomes neither convex nor concave.
3. Non-monotonic behaviour with peaks and/or troughs appear when some of the EoS parameters obey  $w_i > 1/3$ , while others obey  $w_j < 1/3$ .

A schematic illustration of representative spectral morphologies is shown in Fig. 2, where the spectral energy density  $\Omega_{\text{GW}}^{(0)}(f)$  is plotted as a function of the present-day GW frequency  $f$ . The grey-shaded regions indicate approximate detector sensitivity regions (Planck CMB, LISA, aLIGO) and the horizontal dashed line (with reddish shade) schematically marks the BBN constraint. We do not display sensitivity regions of other GW detectors, which were displayed in Ref. [1]. We adhere to the following conventions in all our GW spectral energy density plots—

1. The present-day spectral energy density of inflationary GWs,  $\Omega_{\text{GW}}^{(0)}(f)$ , is plotted as a function of the present-day frequency  $f$ , with both axes in logarithmic scale, as is customary in the literature.

2. The tensor-to-scalar ratio during inflation is fixed at  $r = 0.001$ , which corresponds to an inflationary energy scale of  $E_{\text{inf}} \simeq 5.8 \times 10^{15} \text{ GeV}$  (see App. A.2 of Ref. [1]).
3. The present-day frequency of the tensor mode that re-entered the Hubble radius at the end of inflation can be obtained using Eq. (2.18) as  $f_{\text{end}} \simeq 6.4 \times 10^7 \text{ Hz}$ . We consider this value as the absolute upper limit (UV cut-off) on the GW frequency in all our plots. The lower frequency limit (IR cut-off) is set at  $f_{\text{IR}} \simeq 2 \times 10^{-20} \text{ Hz}$ , corresponding to modes that re-enter the Hubble radius just prior to the onset of the dark energy-dominated accelerated expansion of the Universe.
4. Frequencies corresponding to the transition between successive cosmic epochs are indicated by thin vertical grey lines in all the plots.

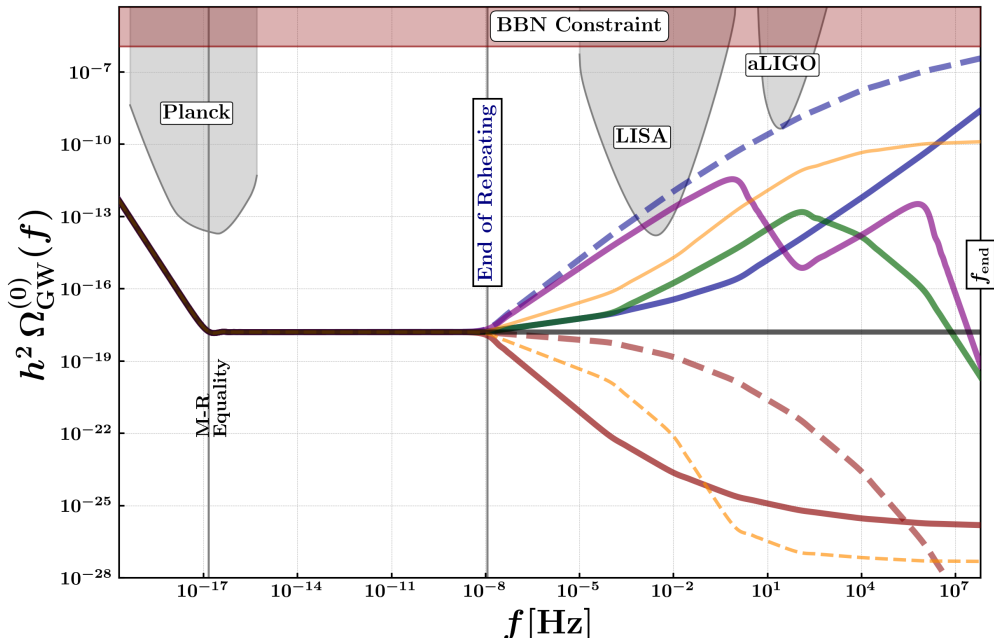


**Figure 2:** Schematic illustration of representative morphologies of the present-day spectral energy density of inflationary gravitational waves,  $\Omega_{\text{GW}}^{(0)}(f)$ , as a function of frequency  $f$  (for various sequences of 7 pre-hot Big Bang epochs after inflation). The solid (dashed) **blue curve** represents a convex (concave), monotonically increasing spectrum arising from a decreasing (increasing) sequence of post-inflationary EoS parameters  $w_1 > w_2 > \dots > w_n$  (for concave the sequence  $w_1 < w_2 < \dots < w_n$ ), corresponding to an overall blue-tilted spectrum. Similarly the solid (dashed) **brown curve** denotes a convex (concave), monotonically decreasing spectrum produced by a decreasing (increasing) sequence of EoS parameters  $w_1 > w_2 > \dots > w_n$  (for concave shape  $w_1 < w_2 < \dots < w_n$ ), resulting in a red-tilted spectrum. Non-monotonic spectra are illustrated by the **green curve** for a single peak and the **purple curve** for two peaks (and a dip). The solid (dashed) **orange curve** corresponds to monotonically increasing (decreasing) spectrum which is neither convex nor concave. The solid **black curve** illustrates an approximately scale-invariant spectrum corresponding to a radiation-like EoS  $w = 1/3$ . The grey-shaded regions indicate the approximate sensitivities of space-based detectors (LISA) and ground-based interferometers (aLIGO), while the red-shaded region marks the BBN constraint. The figure serves to highlight the broad variety of inflationary GW spectral shapes possible for different post-inflationary expansion histories.

### 3.1 Scenarios with monotonic spectra of inflationary gravitational waves

Monotonic spectra of inflationary GWs arise when the sequence of post-inflationary equation-of-state parameters, starting from the first epoch after inflation, evolves to the final epoch prior to the hot Big Bang phase, by remaining either stiffer ( $w_i > 1/3$ ) or softer ( $w_i < 1/3$ ) than a radiation-like EoS  $w = 1/3$ . A sequence of stiffer-than-radiation EoS parameters leads to blue-tilted GW spectrum, while a softer-than-radiation sequence leads to red-tilted GW spectrum, as mentioned before. The commonly assumed scenario of a single constant EoS during the entire post-inflationary evolution is a particular case within this category.

An *increasing* sequence of EoS parameters, *i.e.*,  $w_1 < w_2 < \dots < w_n$ , results in a *concave*-shaped monotonic spectrum of GWs. Conversely, a *decreasing* sequence,  $w_1 > w_2 > \dots > w_n$ , leads to a progressively softer background and produces a *convex*-shaped spectrum. Of particular significance are the blue-tilted spectra of GWs (which may be convex or concave or neither) that arise, when  $w \geq 1/3$ . From a phenomenological standpoint, as it enhances the GW amplitude at higher frequencies, potentially bringing the signal within the sensitivity range of current and upcoming detectors [31, 37, 67], as also discussed extensively in our previous work [1].

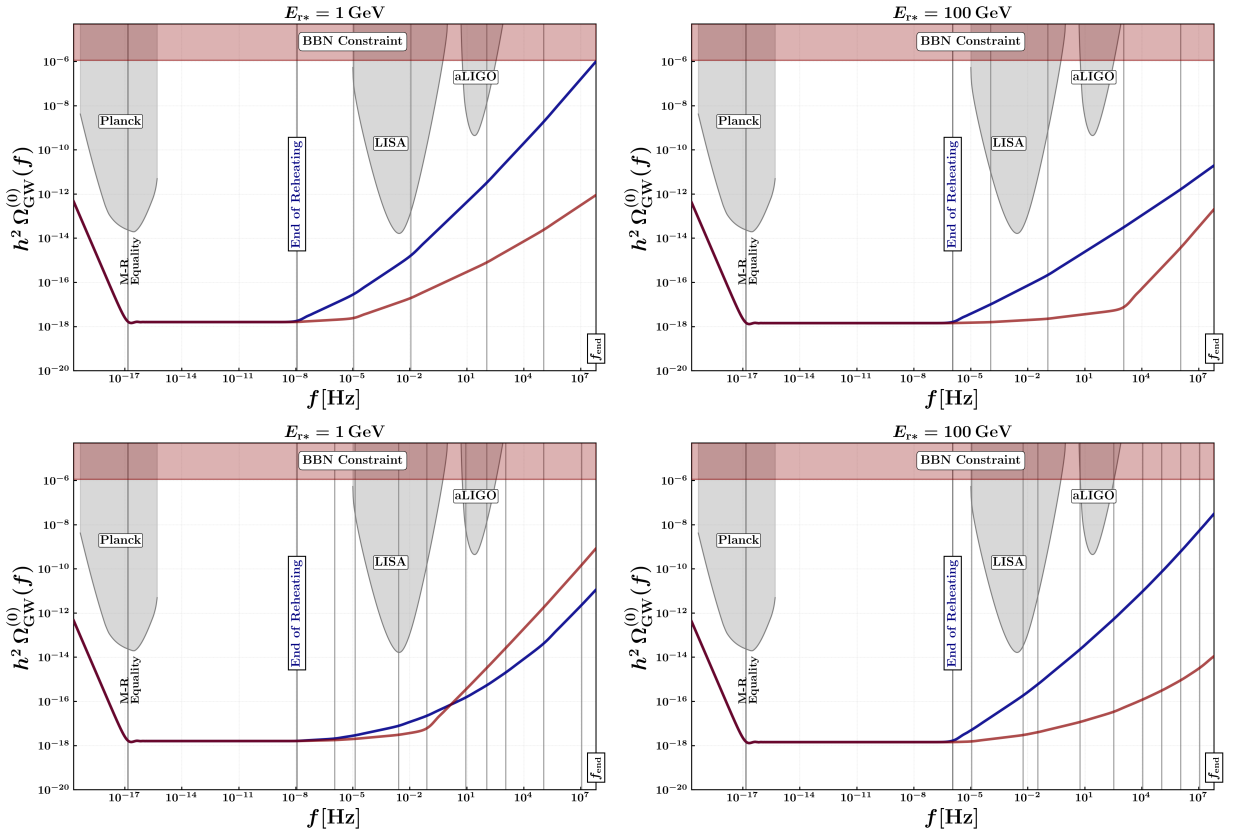


**Figure 3:** Spectral energy density of inflationary GWs,  $\Omega_{\text{GW}}^{(0)}(f)$ , for the case of monotonic blue-tilted, **convex spectra** generated by strictly *decreasing sequences of post-inflationary EoS parameters* ( $w_1 > w_2 > \dots > w_n > w_{\text{rad}} = 1/3$ ). The **top row** contains 5 different post-inflationary epochs, while the **bottom row** contains 10 epochs. The **left column** corresponds to an energy scale of  $E_{\text{r}*} = 1 \text{ GeV}$  at the beginning of hot Big Bang, while the **right column** corresponds to  $E_{\text{r}*} = 100 \text{ GeV}$ . Transitions between successive epochs are marked by grey vertical lines. The BBN constraint is illustrated by the red-shaded region, and the sensitivity curves for LISA, Planck, and aLIGO are displayed by grey-shaded regions. [None of the curves violate the existing constraints from BBN and aLIGO.]

### 3.1.1 Blue-tilted inflationary GWs with convex-shaped spectra

A convex-shaped, monotonically increasing spectrum of inflationary GWs arises when the post-inflationary epochs are characterized by a sequence of progressively softer equations of state,  $w_1 > w_2 > w_3 > \dots > w_{\text{rad}} = 1/3$ . In such scenarios, the spectral energy density  $\Omega_{\text{GW}}^{(0)}(f)$  grows with frequency ( $n_{\text{GW}}(f) > 0$ ), and the rate of growth also gradually increases, *i.e.*,  $[\text{d}/(\text{d} \ln f)] n_{\text{GW}}(f) > 0$ , producing a convex curvature in the  $\log \Omega_{\text{GW}} - \log f$  plane. This behaviour typically originates from the diminishing amplification of the tensor modes as the expansion history transitions from a stiffer to a softer EoS regime. The highest blue tilt results from the first post-inflationary epoch with the stiffest EoS, while the convexity encodes the hierarchical duration and energy scales of the subsequent, softer epochs. A representative class of convex-shaped blue-tilted GW spectra is shown in Fig. 3.

Such convex monotonic spectra are particularly relevant for phenomenological studies, since they can feature a gradual spectral saturation within the frequency bands probed by future space-based interferometers such as LISA, BBO, and DECIGO, with the caveat that a substantial growth of  $\Omega_{\text{GW}}^{(0)}(f)$  at higher frequencies might lead to a violation of the BBN constraint (2.21).

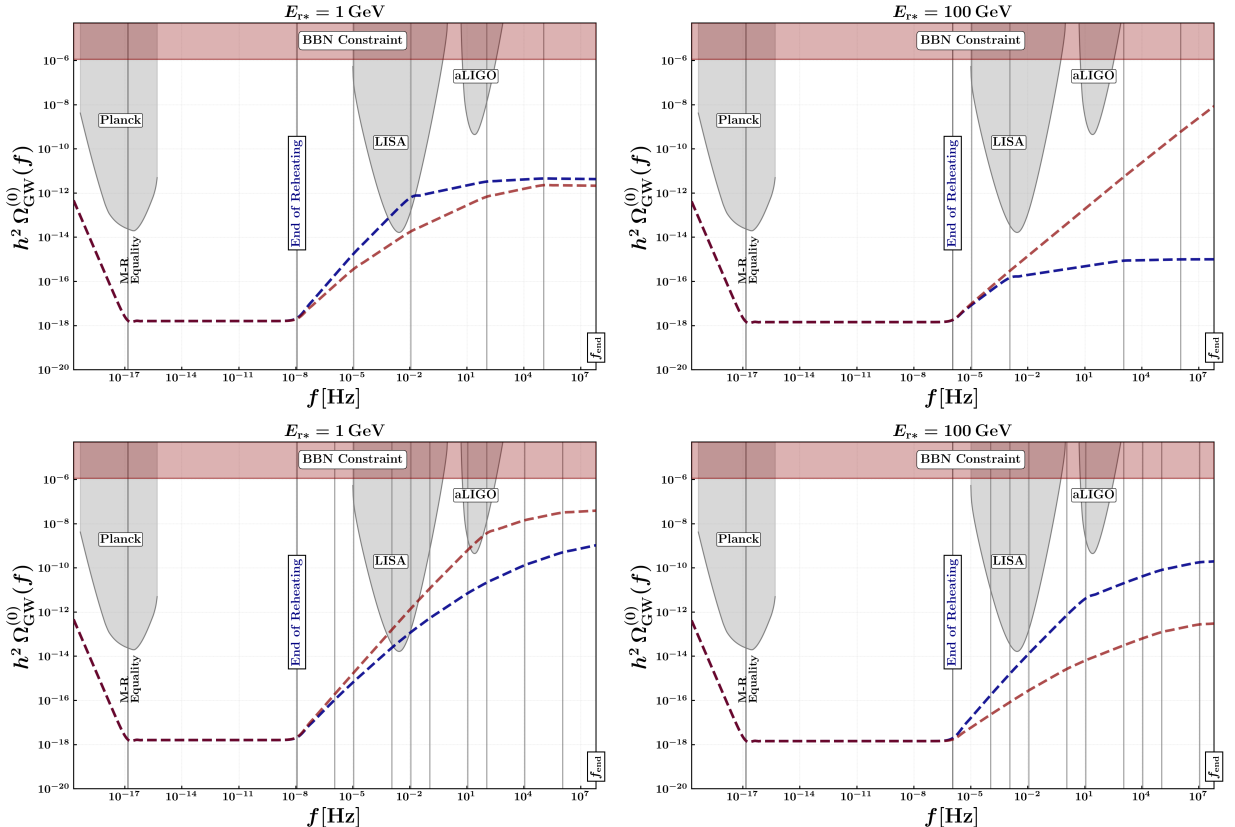


**Figure 4:** Spectral energy density of inflationary GWs,  $\Omega_{\text{GW}}^{(0)}(f)$ , for the case of monotonic blue-tilted, **concave spectra** generated by strictly *increasing sequences of post-inflationary EoS* parameters ( $w_1 < w_2 < \dots < w_n$ ). The **top row** contains 5 different post-inflationary epochs, while the **bottom row** contains 10 epochs. The **left column** corresponds to an energy scale of  $E_{\text{r}*} = 1 \text{ GeV}$  at the beginning of hot Big Bang, while the **right column** corresponds to  $E_{\text{r}*} = 100 \text{ GeV}$ . Transitions between successive epochs are marked by grey vertical lines. The BBN constraint is illustrated by the red-shaded region, and the sensitivity curves for LISA, Planck, and aLIGO are displayed by grey-shaded regions. [None of the curves violate the existing constraints from BBN and aLIGO, except for the red-dashed curve in the bottom-left panel.]

### 3.1.2 Blue-tilted inflationary GWs with concave-shaped spectra

A concave-shaped, monotonically increasing spectrum of inflationary GWs typically results from a post-inflationary expansion history governed by a sequence of increasingly stiffer equations of state,  $w_1 < w_2 < w_3 < \dots < w_n$ . In this case, the spectral energy density  $\Omega_{\text{GW}}^{(0)}(f)$  increases with frequency, exhibiting an overall blue tilt ( $n_{\text{GW}}(f) > 0$ ). However, slope of the spectrum gradually decreases, *i.e.*,  $[d/(d \ln f)] n_{\text{GW}}(f) < 0$ , leading to a concave curvature in the  $\log \Omega_{\text{GW}} - \log f$  plane. A representative class of concave-shaped blue-tilted GW spectra is shown in Fig. 4. Such a spectral shape encodes the gradual hardening of the background EoS—undergoing an ordered sequence of transitions from softer to stiffer dynamics prior to the onset of radiation domination. They also possess a clear phenomenological advantage: their concave shape enables the spectrum to enter the sensitivity bands of space-based (and forthcoming ground-based) detectors at intermediate frequencies, while remaining consistent with the BBN bound due to the gradual flattening of  $\Omega_{\text{GW}}^{(0)}(f)$  at higher frequencies.

## 3.2 Scenarios with non-monotonic spectra of inflationary gravitational waves

In the previous subsection, we focused on monotonically increasing classes of inflationary GW spectra arising from post-inflationary expansion histories characterised by an ordered—either steadily increasing or decreasing—sequence of EoS parameters. In contrast, in the absence of such an ordered sequence of  $\{w_i\}$ , we generically expect non-monotonic features in  $\log \Omega_{\text{GW}}^{(0)}(f) - \log f$  plane.

Such scenarios typically occur when the post-inflationary universe experiences alternating epochs of softer and stiffer equations of state prior to the commencement of the hot Big Bang phase. A gradual transition from softer/stiffer epochs to stiffer/softer epochs imprints a local feature—such as a peak (bump) or a trough (dip)—in the spectral slope of  $\Omega_{\text{GW}}^{(0)}(f)$ . The resulting spectra can thus exhibit multiple turning points, corresponding to characteristic frequencies at which the horizon re-entry of tensor modes coincides with the transition between successive EoS phases. This stands in contrast to the conventional expectation in the literature that inflationary gravitational waves yield strictly monotonic spectra.

In this subsection, we illustrate representative examples of non-monotonic spectra of inflationary GWs, highlighting the variety of shapes that may arise from different sequences of post-inflationary EoS parameters. For concreteness, we restrict our analysis to spectra exhibiting up to two distinct peaks in  $\Omega_{\text{GW}}^{(0)}(f)$ , as these already encompass the essential phenomenology associated with multiple transitions in the equation of state. However, the underlying formalism developed in our previous work [1] and employed here is fully general, and allows the user to construct GW spectra with an arbitrary number of transitions and spectral features<sup>1</sup>. The shapes discussed below therefore serve as templates for understanding how alternating soft and stiff epochs in the post-inflationary history can lead to a rich variety of GW morphologies.

### 3.2.1 Non-monotonic spectra for a soft EoS immediately after inflation

A non-monotonic spectrum can arise when the post-inflationary universe begins with a relatively soft EoS ( $w_1 < 1/3$ ) before transitioning to stiffer or radiation-like epochs. In this case, the early suppression of tensor modes re-entering during the soft phase results in an initial red tilt of  $\Omega_{\text{GW}}^{(0)}(f)$  at high frequencies. Subsequent transitions to larger values of  $w_i$  enhance the spectral slope, producing a local maximum (or bump) at an intermediate frequency corresponding to the scale that re-enters near such transitions. The resulting spectrum therefore exhibits a single or double-peaked profile depending on the number and duration of the subsequent stiff epochs.

---

<sup>1</sup>with the caveat that each epoch must last for at least one  $e$ -fold in order for our analytical approach to remain valid, as discussed in Secs. 2.1 and 4.2.

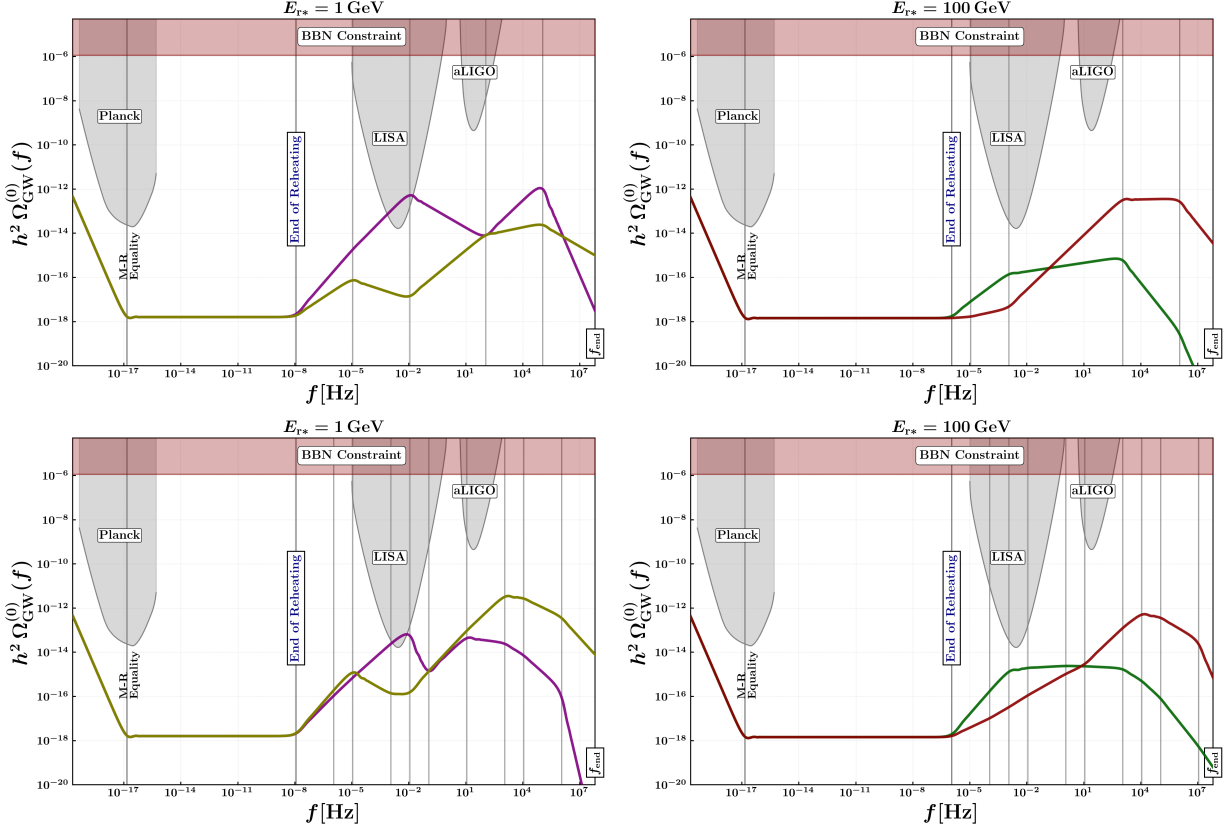


**Figure 5:** Spectral energy density of inflationary GWs,  $\Omega_{\text{GW}}^{(0)}(f)$ , for the case of **non-monotonic spectra with peak(s)**, arising when the post-inflationary universe begins with a softer EoS ( $w_1 < 1/3$ ), but later evolves to become stiffer ( $w > 1/3$ ) at some epoch. The **top row** contains 5 different post-inflationary epochs, while the **bottom row** contains 10 epochs. The **left column** corresponds to an energy scale of  $E_{\text{r}*} = 1 \text{ GeV}$  at the beginning of hot Big Bang, while the **right column** corresponds to  $E_{\text{r}*} = 100 \text{ GeV}$ . Transitions between successive epochs are marked by grey vertical lines. The BBN constraint is illustrated by the red-shaded region, and the sensitivity curves for LISA, Planck, and aLIGO are displayed by grey-shaded regions. [None of the curves violate the existing constraints from BBN and aLIGO.]

Physically, this behaviour reflects the temporary dilution of GW energy density during the soft phase(s), followed by a relative amplification in the stiff epoch(s). A representative class of non-monotonic GW spectra with  $w_1 < 1/3$  is shown in Fig. 5.

### 3.2.2 Non-monotonic spectra for a stiff EoS immediately after inflation

Conversely, if the universe initially enters a stiff post-inflationary epoch ( $w_1 > 1/3$ ), including a brief kination phase, the corresponding GW spectrum exhibits an opposite sequence of features. The early blue tilt, generated by the rapid dilution of the background energy density during the stiff epoch, enhances  $\Omega_{\text{GW}}^{(0)}(f)$  at high frequencies, which is associated with modes making an early horizon re-entry.

When the universe subsequently transitions to a softer phase ( $w_{(i>1)} < w_1$ ), the spectral slope decreases, producing a turnover that manifests as a suppression, some times as a trough (or dip) at intermediate frequencies. This generates a non-monotonic structure characterised by one or more peaks depending on the number of alternating stiff–soft transitions. A representative class of non-monotonic GW spectra with  $w_1 > 1/3$  is shown in Fig. 6.

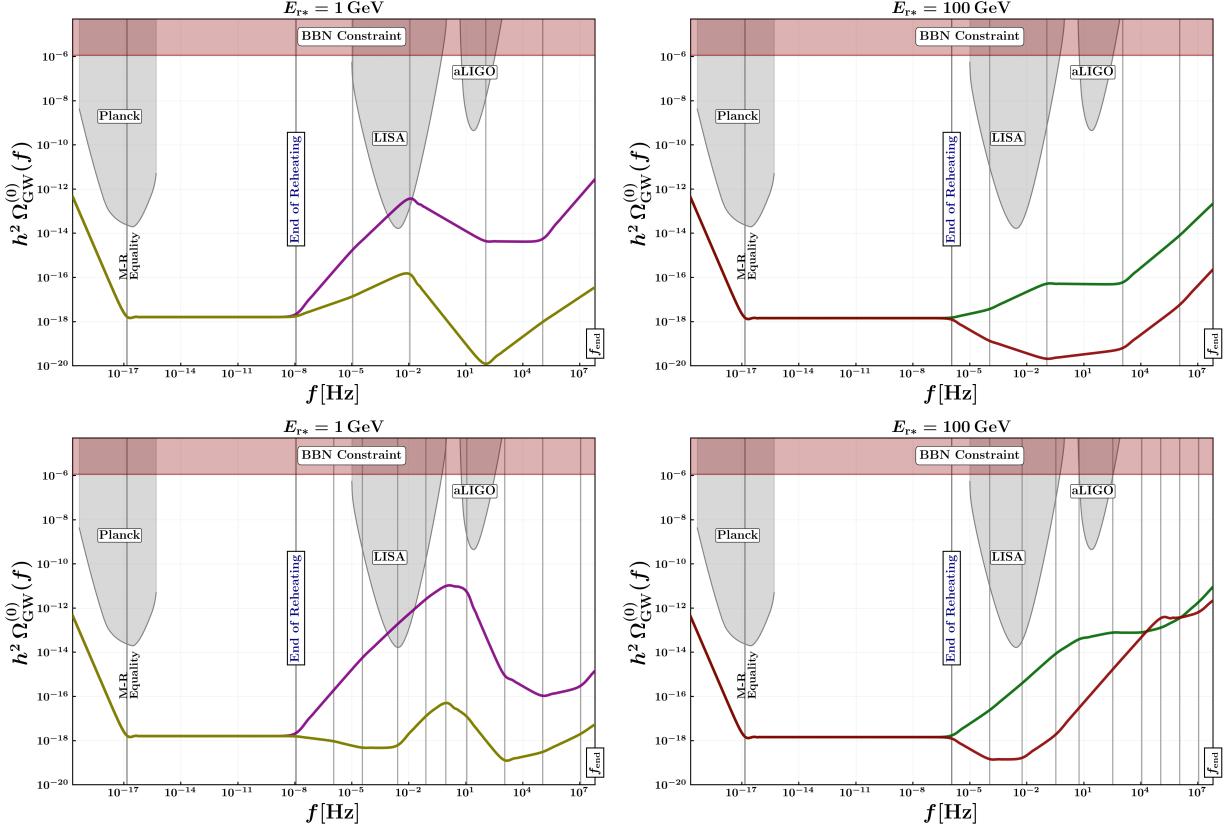


**Figure 6:** Spectral energy density of inflationary GWs,  $\Omega_{\text{GW}}^{(0)}(f)$ , for the case of **non-monotonic spectra**, arising when the post-inflationary universe begins with a stiffer EoS ( $w_1 > 1/3$ ), but later evolves to become softer ( $w < 1/3$ ) at some epoch. The **top row** contains 5 different post-inflationary epochs, while the **bottom row** contains 10 epochs. The **left column** corresponds to an energy scale of  $E_{\text{r}*} = 1 \text{ GeV}$  at the beginning of hot Big Bang, while the **right column** corresponds to  $E_{\text{r}*} = 100 \text{ GeV}$ . Transitions between successive epochs are marked by grey vertical lines. The BBN constraint is illustrated by the red-shaded region, and the sensitivity curves for LISA, Planck, and aLIGO are displayed by grey-shaded regions. [None of the curves violate the existing constraints from BBN and aLIGO.]

Primordial GWs with both the aforementioned types of non-monotonic spectra, with one or more peaks, are particularly interesting from a phenomenological perspective, since they can yield enhanced power in frequency bands accessible to space-based and/or ground-based GW detectors, while still remaining consistent with the BBN constraints.

## 4 GWInSpect: Python-based numerical package

### 4.1 Overview

GWInSpect  is a Python-based numerical framework designed to compute the present-day spectral energy density of inflationary gravitational waves,  $\Omega_{\text{GW}}^{(0)}(f)$ , for a user-specified post-inflationary expansion history consisting of multiple epochs with instantaneous transitions. Each epoch is characterized by a constant equation-of-state parameter, and the code implements the junction matching conditions described in Ref. [1] to evolve the tensor modes across successive epochs.

The package is lightweight, modular, and written for both exploratory and precision studies of the inflationary GW background. It employs the following major libraries:

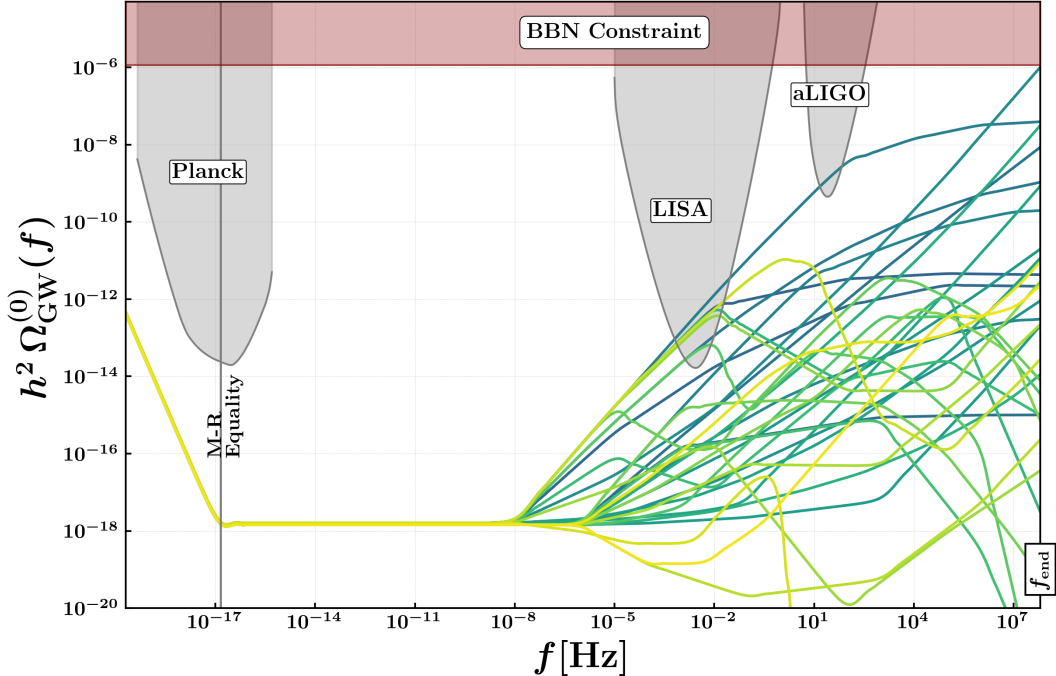


**Figure 7: Spectral zoo plot** illustrating a variety of possible morphologies of the inflationary GW spectra  $\Omega_{\text{GW}}^{(0)}(f)$ , generated by stacking together all the curves appearing in Figs. 3–6 (with the colour scheme corresponding to the order in which we plotted all the curves from Fig. 3 to Fig. 6, without any physical significance).

- **NumPy:** Array programming and vectorized numerical computing for scientific workflows [78].
- **SciPy:** Used the special function Gamma [79].
- **mpmath:** For high-precision evaluations of Bessel functions, ensuring numerical stability in oscillatory regimes [80].

## 4.2 Required inputs

The following inputs are required to run `GWInSpect`. Unless otherwise stated, any input lying outside the specified range is automatically rejected with a descriptive message.

- **List of EoS parameters:**  $\{w_1, w_2, \dots, w_n\}$ , ordered from the earliest to the latest post-inflationary epoch, satisfying  $-0.28 \leq w_i < 1$ .
- **Transition energies:** An ascending list  $\{E_{n-1}, \dots, E_1\}$  in GeV, defining the boundaries between epochs (latest  $\rightarrow$  earliest). The typical range is  $10^{-3} \text{ GeV} \lesssim E_i \lesssim 10^{16} \text{ GeV}$ . The terminal hot Big Bang energy scale  $E_{\text{r}*}$  is not included in this list.
- **Commencement of hot Big Bang:** Either specify the hot Big Bang temperature  $T_{\text{r}*} \geq 10^{-3} \text{ GeV}$  (consistent with BBN constraints) or the corresponding energy scale  $E_{\text{r}*}$ , which the code internally maps to  $T_{\text{r}*}$ .
- **Inflationary scale:** Specify either the tensor-to-scalar ratio  $r$  (restricted to  $r < 0.036$ ) or the corresponding energy scale of inflation,  $E_{\text{inf}} < 1.4 \times 10^{16} \text{ GeV}$ .

### Duration of each epoch.

To maintain the validity of the instantaneous-transition approximation discussed in Sec. 2.1, **GWInSpect** enforces that every post-inflationary epoch must span at least one  $e$ -fold. The number of  $e$ -folds in the  $i^{\text{th}}$  epoch is defined as

$$\boxed{\Delta N_i = \frac{4}{3(1 + w_i)} \ln\left(\frac{E_{i-1}}{E_i}\right)} \geq 1 \quad \forall i \in \{1, 2, \dots, n\}. \quad (4.1)$$

If  $\Delta N_i < 1$  for any epoch, the code halts execution and prompts the user to revise the duration (energy hierarchy) or the EoS parameters of the input sequence. For transparency, the complete array  $\{\Delta N_i\}$  can also be given as one of the output for user inspection.

### 4.3 Typical outputs

**GWInSpect** produces the following key outputs :

- A log-spaced frequency array covering the range from the infrared cut-off to the UV cut-off, i.e.  $f_{\text{IR}}$  to  $f_{\text{end}}$ .
- The corresponding present-day spectral energy density array,  $\Omega_{\text{GW}}^{(0)}(f)$ .
- A list of present-day frequencies corresponding to the Hubble re-entry times of the tensor modes at each instantaneous transition (including  $f_{\text{end}}$  as the first entry) (optional).
- A list of the number of  $e$ -folds  $\{\Delta N_i\}$  associated with each post-inflationary epoch (optional).

Together, these outputs enable the user to reconstruct the full morphology of the inflationary GW spectra and study its dependence on the hitherto unknown expansion history of the early Universe<sup>2</sup>. We provide an instructive tutorial with an `ipynb` notebook for the reader, which can be directly accessed from the link: [tutorial notebook](#).

## 5 Discussion and Outlook

In this work, employing the analytical framework developed in our previous paper [1] for computing the present-day spectral energy density of first-order inflationary GWs,  $\Omega_{\text{GW}}^{(0)}(f)$ , we carried out a systematic investigation of their spectral shapes. A key methodological distinction of this work is its focus on the *morphological diversity* of the inflationary GW spectra, including monotonic (red-tilted or blue-tilted, convex or concave) and non-monotonic (single-peaked or multi-peaked) forms, rather than on detection prospects or parameter constraints, which were the main objectives of Ref. [1].

These distinct morphologies naturally emerge from different combinations of cosmic epochs, with soft and stiff post-inflationary EoS parameters, preceding the onset of the hot Big Bang phase. The analytical formalism developed in [1], employing Israel junction conditions and the Heaviside representation of sharp transitions, is directly applied here to study the possible shapes of  $\Omega_{\text{GW}}^{(0)}(f)$  across multiple post-inflationary epochs. Apart from the BBN constraints on GWs, we enforce the condition that each post-inflationary epoch lasts at least one  $e$ -fold, thereby preserving the validity of the instantaneous-transition approximation underlying our analytical approach. Our analysis remains entirely model-agnostic, relying only on the sequence of EoS parameters without invoking any specific microphysical or particle-physics realization.

<sup>2</sup>We also make available a list of useful additional functions within this package, such as the ones to check the BBN constraint using Eq. (2.21) and to relate different early Universe quantities at a certain epoch, amongst others.

A complementary aim of this study is the development of a practical, user-friendly numerical package, **GWInSpect**, which automates the computation of  $\Omega_{\text{GW}}^{(0)}(f)$  for arbitrary sequences of the post-inflationary EoS parameters and the corresponding transition energy scales. The publicly available code provides a fast and flexible tool for generating GW spectra corresponding to a wide range of post-inflationary histories. In this way, **GWInSpect** bridges the analytical formalism of [1] with numerical implementation, enabling efficient exploration of early-Universe reheating scenarios. Together, these two studies provide a simple computational framework for probing the unknown history of the early Universe through the imprints of its post-inflationary dynamics on the inflationary GW background.

Looking ahead, there exist several promising directions in which the present framework can be extended and refined.

- As in our previous work, the analytical framework developed across these two studies can be readily employed for model-dependent analyses, enabling one to constrain the underlying physical parameters of specific post-inflationary scenarios [81] in light of present and future GW observational prospects.
- By relaxing the requirement that each post-inflationary epoch must last at least one  $e$ -fold, through the incorporation of smooth transitions (implemented via suitable functional forms) between successive epochs, one can achieve a more realistic and fine-grained characterization of the underlying cosmological dynamics.
- A long-term goal is to extend the present formalism to study the impact of multiple post-inflationary transitions on the spectra of *scalar-induced gravitational waves* (SIGWs) [76, 82–84]. Since such second-order GWs depend greatly on the background expansion history, the analytical and numerical techniques developed here can offer valuable insights into their spectral structure.

## 6 Acknowledgements

We thank Mohammed Shafi and Siddharth Bhatt for valuable discussions and for carefully reading the draft and providing helpful comments. We also thank Sanket Dave for locating typos in the draft. A substantial portion of this work was carried out at IUCAA, for which SSM gratefully acknowledges support from the IUCAA Visitor Academic Programme. Insightful discussions with Ed Copeland, Varun Sahni, Oliver Gould, Sanjit Mitra and Ranjeev Misra on gravitational waves over the years have been helpful in shaping this work. SSM was supported by the STFC Consolidated Grant [ST/T000732/1] at the University of Nottingham. AKS acknowledges funding support from SISSA as a PhD student.

**Data Availability Statement:** This work is entirely theoretical and has no associated data. The Python package **GWInSpect** developed to compute the spectral energy density of first-order inflationary GWs can be found in our [GitHub repository](#) , with a [tutorial notebook](#).

**AI Assistance Statement:** The authors acknowledge the use of **ChatGPT** (OpenAI GPT-5) for language editing and stylistic refinement of the manuscript.

For the purpose of open access, the authors have applied a CC BY public copyright license to any Author Accepted Manuscript version arising.

## References

- [1] Athul K. Soman et al. “Inflationary Gravitational Waves as a probe of the unknown post-inflationary primordial Universe”. In: (July 2024). arXiv: [2407.07956 \[gr-qc\]](https://arxiv.org/abs/2407.07956).
- [2] Alexei A. Starobinsky. “A New Type of Isotropic Cosmological Models Without Singularity”. In: *Phys. Lett. B* 91 (1980). Ed. by I. M. Khalatnikov and V. P. Mineev, pp. 99–102. DOI: [10.1016/0370-2693\(80\)90670-X](https://doi.org/10.1016/0370-2693(80)90670-X).
- [3] Alan H. Guth. “The Inflationary Universe: A Possible Solution to the Horizon and Flatness Problems”. In: *Phys. Rev. D* 23 (1981). Ed. by Li-Zhi Fang and R. Ruffini, pp. 347–356. DOI: [10.1103/PhysRevD.23.347](https://doi.org/10.1103/PhysRevD.23.347).
- [4] Andrei D. Linde. “A New Inflationary Universe Scenario: A Possible Solution of the Horizon, Flatness, Homogeneity, Isotropy and Primordial Monopole Problems”. In: *Phys. Lett. B* 108 (1982). Ed. by Li-Zhi Fang and R. Ruffini, pp. 389–393. DOI: [10.1016/0370-2693\(82\)91219-9](https://doi.org/10.1016/0370-2693(82)91219-9).
- [5] Andreas Albrecht and Paul J. Steinhardt. “Cosmology for Grand Unified Theories with Radiatively Induced Symmetry Breaking”. In: *Phys. Rev. Lett.* 48 (1982). Ed. by Li-Zhi Fang and R. Ruffini, pp. 1220–1223. DOI: [10.1103/PhysRevLett.48.1220](https://doi.org/10.1103/PhysRevLett.48.1220).
- [6] Andrei D. Linde. “Chaotic Inflation”. In: *Phys. Lett. B* 129 (1983), pp. 177–181. DOI: [10.1016/0370-2693\(83\)90837-7](https://doi.org/10.1016/0370-2693(83)90837-7).
- [7] Andrei D. Linde. *Particle physics and inflationary cosmology*. Vol. 5. 1990. arXiv: [hep-th/0503203](https://arxiv.org/abs/hep-th/0503203).
- [8] William H. Kinney. *TASI Lectures on Inflation*. 2009. arXiv: [0902.1529 \[astro-ph.CO\]](https://arxiv.org/abs/0902.1529).
- [9] Jerome Martin, Christophe Ringeval, and Vincent Vennin. “Encyclopædia Inflationaris”. In: *Phys. Dark Univ.* 5-6 (2014), pp. 75–235. DOI: [10.1016/j.dark.2014.01.003](https://doi.org/10.1016/j.dark.2014.01.003). arXiv: [1303.3787 \[astro-ph.CO\]](https://arxiv.org/abs/1303.3787).
- [10] Daniel Baumann. “Inflation”. In: *Theoretical Advanced Study Institute in Elementary Particle Physics: Physics of the Large and the Small*. 2011, pp. 523–686. DOI: [10.1142/9789814327183\\_0010](https://doi.org/10.1142/9789814327183_0010). arXiv: [0907.5424 \[hep-th\]](https://arxiv.org/abs/0907.5424).
- [11] Daniel Baumann. “Primordial Cosmology”. In: *PoS TASI2017* (2018), p. 009. DOI: [10.22323/1.305.0009](https://doi.org/10.22323/1.305.0009). arXiv: [1807.03098 \[hep-th\]](https://arxiv.org/abs/1807.03098).
- [12] Hideo Kodama and Misao Sasaki. “Cosmological Perturbation Theory”. In: *Progress of Theoretical Physics Supplement* 78 (Jan. 1984), pp. 1–166. ISSN: 0375-9687. DOI: [10.1143/PTPS.78.1](https://doi.org/10.1143/PTPS.78.1). eprint: <https://academic.oup.com/ptps/article-pdf/doi/10.1143/PTPS.78.1/5321391/78-1.pdf>. URL: <https://doi.org/10.1143/PTPS.78.1>.
- [13] Antonio Riotto. “Inflation and the theory of cosmological perturbations”. In: *ICTP Lect. Notes Ser.* 14 (2003). Ed. by G. Dvali et al., pp. 317–413. arXiv: [hep-ph/0210162](https://arxiv.org/abs/hep-ph/0210162).
- [14] John Ellis and David Wands. “Inflation (2023)”. In: (Dec. 2023). arXiv: [2312.13238 \[astro-ph.CO\]](https://arxiv.org/abs/2312.13238).
- [15] Swagat S. Mishra. “Cosmic Inflation: Background dynamics, Quantum fluctuations and Re-heating”. Other thesis. Mar. 2024. arXiv: [2403.10606 \[gr-qc\]](https://arxiv.org/abs/2403.10606).
- [16] Edward W. Kolb and Michael S. Turner. *The Early Universe*. Vol. 69. 1990. ISBN: 978-0-201-62674-2. DOI: [10.1201/9780429492860](https://doi.org/10.1201/9780429492860).
- [17] Scott Dodelson. *Modern Cosmology*. Amsterdam: Academic Press, 2003. ISBN: 978-0-12-219141-1.
- [18] Valery A. Rubakov and Dmitry S. Gorbunov. *Introduction to the Theory of the Early Universe: Hot big bang theory*. Singapore: World Scientific, 2017. ISBN: 978-981-320-987-9. DOI: [10.1142/10447](https://doi.org/10.1142/10447).

[19] Viatcheslav F. Mukhanov and G. V. Chibisov. “Quantum Fluctuations and a Nonsingular Universe”. In: *JETP Lett.* 33 (1981), pp. 532–535.

[20] S. W. Hawking. “The Development of Irregularities in a Single Bubble Inflationary Universe”. In: *Phys. Lett. B* 115 (1982), p. 295. DOI: [10.1016/0370-2693\(82\)90373-2](https://doi.org/10.1016/0370-2693(82)90373-2).

[21] Alexei A. Starobinsky. “Dynamics of Phase Transition in the New Inflationary Universe Scenario and Generation of Perturbations”. In: *Phys. Lett. B* 117 (1982), pp. 175–178. DOI: [10.1016/0370-2693\(82\)90541-X](https://doi.org/10.1016/0370-2693(82)90541-X).

[22] Alan H. Guth and S. Y. Pi. “Fluctuations in the New Inflationary Universe”. In: *Phys. Rev. Lett.* 49 (1982), pp. 1110–1113. DOI: [10.1103/PhysRevLett.49.1110](https://doi.org/10.1103/PhysRevLett.49.1110).

[23] N. Aghanim et al. “Planck 2018 results. VI. Cosmological parameters”. In: *Astron. Astrophys.* 641 (2020). [Erratum: *Astron. Astrophys.* 652, C4 (2021)], A6. DOI: [10.1051/0004-6361/201833910](https://doi.org/10.1051/0004-6361/201833910). arXiv: [1807.06209 \[astro-ph.CO\]](https://arxiv.org/abs/1807.06209).

[24] N. Aghanim et al. “Planck 2018 results. I. Overview and the cosmological legacy of Planck”. In: *Astron. Astrophys.* 641 (2020), A1. DOI: [10.1051/0004-6361/201833880](https://doi.org/10.1051/0004-6361/201833880). arXiv: [1807.06205 \[astro-ph.CO\]](https://arxiv.org/abs/1807.06205).

[25] Y. Akrami et al. “Planck 2018 results. X. Constraints on inflation”. In: *Astron. Astrophys.* 641 (2020), A10. DOI: [10.1051/0004-6361/201833887](https://doi.org/10.1051/0004-6361/201833887). arXiv: [1807.06211 \[astro-ph.CO\]](https://arxiv.org/abs/1807.06211).

[26] P. A. R. Ade et al. “Improved Constraints on Primordial Gravitational Waves using Planck, WMAP, and BICEP/Keck Observations through the 2018 Observing Season”. In: *Phys. Rev. Lett.* 127.15, 151301 (Oct. 2021), p. 151301. DOI: [10.1103/PhysRevLett.127.151301](https://doi.org/10.1103/PhysRevLett.127.151301). arXiv: [2110.00483 \[astro-ph.CO\]](https://arxiv.org/abs/2110.00483).

[27] V. Mukhanov. *Physical Foundations of Cosmology*. Oxford: Cambridge University Press, 2005. ISBN: 978-0-521-56398-7. DOI: [10.1017/CBO9780511790553](https://doi.org/10.1017/CBO9780511790553).

[28] Daniel Baumann. *Cosmology*. Cambridge University Press, July 2022. ISBN: 978-1-108-93709-2. DOI: [10.1017/9781108937092](https://doi.org/10.1017/9781108937092).

[29] L. P. Grishchuk. “Amplification of gravitational waves in an istropic universe”. In: *Zh. Eksp. Teor. Fiz.* 67 (1974), pp. 825–838.

[30] Alexei A. Starobinsky. “Spectrum of relict gravitational radiation and the early state of the universe”. In: *JETP Lett.* 30 (1979). Ed. by I. M. Khalatnikov and V. P. Mineev, pp. 682–685.

[31] Varun Sahni. “The Energy Density of Relic Gravity Waves From Inflation”. In: *Phys. Rev. D* 42 (1990), pp. 453–463. DOI: [10.1103/PhysRevD.42.453](https://doi.org/10.1103/PhysRevD.42.453).

[32] Bruce Allen. “The Stochastic Gravity Wave Background in Inflationary Universe Models”. In: *Phys. Rev. D* 37 (1988), p. 2078. DOI: [10.1103/PhysRevD.37.2078](https://doi.org/10.1103/PhysRevD.37.2078).

[33] Massimo Giovannini. “Stochastic gravitational waves backgrounds: a probe for inflationary and non-inflationary cosmology”. In: *3rd International Conference on Particle Physics and the Early Universe*. 2000, pp. 167–173. DOI: [10.1142/9789812792129\\_0024](https://doi.org/10.1142/9789812792129_0024). arXiv: [hep-ph/9912480](https://arxiv.org/abs/hep-ph/9912480).

[34] Swagat S. Mishra, Varun Sahni, and Alexei A. Starobinsky. “Curing inflationary degeneracies using reheating predictions and relic gravitational waves”. In: *JCAP* 05 (2021), p. 075. DOI: [10.1088/1475-7516/2021/05/075](https://doi.org/10.1088/1475-7516/2021/05/075). arXiv: [2101.00271 \[gr-qc\]](https://arxiv.org/abs/2101.00271).

[35] Md Riajul Haque et al. “Decoding the phases of early and late time reheating through imprints on primordial gravitational waves”. In: *Phys. Rev. D* 104.6 (2021), p. 063513. DOI: [10.1103/PhysRevD.104.063513](https://doi.org/10.1103/PhysRevD.104.063513). arXiv: [2105.09242 \[astro-ph.CO\]](https://arxiv.org/abs/2105.09242).

[36] Massimo Giovannini. “Primordial backgrounds of relic gravitons”. In: *Prog. Part. Nucl. Phys.* 112 (2020), p. 103774. DOI: [10.1016/j.ppnp.2020.103774](https://doi.org/10.1016/j.ppnp.2020.103774). arXiv: [1912.07065 \[astro-ph.CO\]](https://arxiv.org/abs/1912.07065).

[37] Chiara Caprini and Daniel G. Figueroa. “Cosmological Backgrounds of Gravitational Waves”. In: *Class. Quant. Grav.* 35.16 (2018), p. 163001. doi: [10.1088/1361-6382/aac608](https://doi.org/10.1088/1361-6382/aac608). arXiv: [1801.04268 \[astro-ph.CO\]](https://arxiv.org/abs/1801.04268).

[38] M. C. Guzzetti et al. “Gravitational waves from inflation”. In: *Riv. Nuovo Cim.* 39.9 (2016), pp. 399–495. doi: [10.1393/ncr/i2016-10127-1](https://doi.org/10.1393/ncr/i2016-10127-1). arXiv: [1605.01615 \[astro-ph.CO\]](https://arxiv.org/abs/1605.01615).

[39] Yu-Tong Wang et al. “Probing the primordial universe with gravitational waves detectors”. In: *JCAP* 01 (2017), p. 010. doi: [10.1088/1475-7516/2017/01/010](https://doi.org/10.1088/1475-7516/2017/01/010). arXiv: [1612.05088 \[astro-ph.CO\]](https://arxiv.org/abs/1612.05088).

[40] Benjamin Racine et al. “Measurements of Degree-Scale B-mode Polarization with the BICEP/Keck Experiments at South Pole”. In: *53rd Rencontres de Moriond on Cosmology*. 2018, pp. 113–120. arXiv: [1807.02199 \[astro-ph.CO\]](https://arxiv.org/abs/1807.02199).

[41] M. Hazumi et al. “LiteBIRD: A Satellite for the Studies of B-Mode Polarization and Inflation from Cosmic Background Radiation Detection”. In: *J. Low Temp. Phys.* 194.5-6 (2019), pp. 443–452. doi: [10.1007/s10909-019-02150-5](https://doi.org/10.1007/s10909-019-02150-5).

[42] A. Suzuki et al. “The POLARBEAR-2 and the Simons Array Experiment”. In: *J. Low Temp. Phys.* 184.3-4 (2016). Ed. by Philippe Camus, Alexandre Juillard, and Alessandro Monfardini, pp. 805–810. doi: [10.1007/s10909-015-1425-4](https://doi.org/10.1007/s10909-015-1425-4). arXiv: [1512.07299 \[astro-ph.IM\]](https://arxiv.org/abs/1512.07299).

[43] Gabriella Agazie et al. “The NANOGrav 15 yr Data Set: Evidence for a Gravitational-wave Background”. In: *Astrophys. J. Lett.* 951.1 (2023), p. L8. doi: [10.3847/2041-8213/acdac6](https://doi.org/10.3847/2041-8213/acdac6). arXiv: [2306.16213 \[astro-ph.HE\]](https://arxiv.org/abs/2306.16213).

[44] Gabriella Agazie et al. “The NANOGrav 15 yr Data Set: Search for Anisotropy in the Gravitational-wave Background”. In: *Astrophys. J. Lett.* 956.1 (2023), p. L3. doi: [10.3847/2041-8213/acf4fd](https://doi.org/10.3847/2041-8213/acf4fd). arXiv: [2306.16221 \[astro-ph.HE\]](https://arxiv.org/abs/2306.16221).

[45] J. Antoniadis et al. “The second data release from the European Pulsar Timing Array - III. Search for gravitational wave signals”. In: *Astron. Astrophys.* 678 (2023), A50. doi: [10.1051/0004-6361/202346844](https://doi.org/10.1051/0004-6361/202346844). arXiv: [2306.16214 \[astro-ph.HE\]](https://arxiv.org/abs/2306.16214).

[46] J. Antoniadis et al. “The second data release from the European Pulsar Timing Array - I. The dataset and timing analysis”. In: *Astron. Astrophys.* 678 (2023), A48. doi: [10.1051/0004-6361/202346841](https://doi.org/10.1051/0004-6361/202346841). arXiv: [2306.16224 \[astro-ph.HE\]](https://arxiv.org/abs/2306.16224).

[47] G. Agazie et al. “Comparing Recent Pulsar Timing Array Results on the Nanohertz Stochastic Gravitational-wave Background”. In: *Astrophys. J.* 966.1 (2024), p. 105. doi: [10.3847/1538-4357/ad36be](https://doi.org/10.3847/1538-4357/ad36be). arXiv: [2309.00693 \[astro-ph.HE\]](https://arxiv.org/abs/2309.00693).

[48] J. Aasi et al. “Advanced LIGO”. In: *Class. Quant. Grav.* 32 (2015), p. 074001. doi: [10.1088/0264-9381/32/7/074001](https://doi.org/10.1088/0264-9381/32/7/074001). arXiv: [1411.4547 \[gr-qc\]](https://arxiv.org/abs/1411.4547).

[49] F. Acernese et al. “Advanced Virgo: a second-generation interferometric gravitational wave detector”. In: *Class. Quant. Grav.* 32.2 (2015), p. 024001. doi: [10.1088/0264-9381/32/2/024001](https://doi.org/10.1088/0264-9381/32/2/024001). arXiv: [1408.3978 \[gr-qc\]](https://arxiv.org/abs/1408.3978).

[50] T. Akutsu et al. “KAGRA: 2.5 Generation Interferometric Gravitational Wave Detector”. In: *Nature Astron.* 3.1 (2019), pp. 35–40. doi: [10.1038/s41550-018-0658-y](https://doi.org/10.1038/s41550-018-0658-y). arXiv: [1811.08079 \[gr-qc\]](https://arxiv.org/abs/1811.08079).

[51] Pau Amaro-Seoane et al. “Laser Interferometer Space Antenna”. In: (Feb. 2017). arXiv: [1702.00786 \[astro-ph.IM\]](https://arxiv.org/abs/1702.00786).

[52] Seiji Kawamura. “Primordial gravitational wave and DECIGO”. In: *PoS KMI2019* (2019), p. 019. doi: [10.22323/1.356.0019](https://doi.org/10.22323/1.356.0019).

[53] G. M. Harry et al. “Laser interferometry for the big bang observer”. In: *Class. Quant. Grav.* 23 (2006). [Erratum: *Class.Quant.Grav.* 23, 7361 (2006)], pp. 4887–4894. DOI: [10.1088/0264-9381/23/15/008](https://doi.org/10.1088/0264-9381/23/15/008).

[54] David Reitze et al. “Cosmic Explorer: The U.S. Contribution to Gravitational-Wave Astronomy beyond LIGO”. In: *Bull. Am. Astron. Soc.* 51.7 (2019), p. 035. arXiv: [1907.04833 \[astro-ph.IM\]](https://arxiv.org/abs/1907.04833).

[55] Eugenio Coccia. “The Einstein Telescope”. In: *PoS* ICRC2023 (2024), p. 1591. DOI: [10.22323/1.444.1591](https://doi.org/10.22323/1.444.1591).

[56] Lev Kofman, Andrei D. Linde, and Alexei A. Starobinsky. “Towards the theory of reheating after inflation”. In: *Phys. Rev. D* 56 (1997), pp. 3258–3295. DOI: [10.1103/PhysRevD.56.3258](https://doi.org/10.1103/PhysRevD.56.3258). arXiv: [hep-ph/9704452](https://arxiv.org/abs/hep-ph/9704452).

[57] Kaloian D. Lozanov. “Lectures on Reheating after Inflation”. In: (July 2019). arXiv: [1907.04402 \[astro-ph.CO\]](https://arxiv.org/abs/1907.04402).

[58] Mustafa A. Amin et al. “Nonperturbative Dynamics Of Reheating After Inflation: A Review”. In: *Int. J. Mod. Phys. D* 24 (2014), p. 1530003. DOI: [10.1142/S0218271815300037](https://doi.org/10.1142/S0218271815300037). arXiv: [1410.3808 \[hep-ph\]](https://arxiv.org/abs/1410.3808).

[59] Rouzbeh Allahverdi et al. “The First Three Seconds: a Review of Possible Expansion Histories of the Early Universe”. In: (June 2020). DOI: [10.21105/astro.2006.16182](https://doi.org/10.21105/astro.2006.16182). arXiv: [2006.16182 \[astro-ph.CO\]](https://arxiv.org/abs/2006.16182).

[60] Massimo Giovannini. “Relic gravitons at intermediate frequencies and the expansion history of the Universe”. In: *Phys. Rev. D* 105.10 (2022), p. 103524. DOI: [10.1103/PhysRevD.105.103524](https://doi.org/10.1103/PhysRevD.105.103524). arXiv: [2203.13586 \[gr-qc\]](https://arxiv.org/abs/2203.13586).

[61] Yann Gouttenoire, Geraldine Servant, and Peera Simakachorn. “Kination cosmology from scalar fields and gravitational-wave signatures”. In: (Nov. 2021). arXiv: [2111.01150 \[hep-ph\]](https://arxiv.org/abs/2111.01150).

[62] Yann Gouttenoire, Géraldine Servant, and Peera Simakachorn. “Beyond the Standard Models with Cosmic Strings”. In: *JCAP* 07 (2020), p. 032. DOI: [10.1088/1475-7516/2020/07/032](https://doi.org/10.1088/1475-7516/2020/07/032). arXiv: [1912.02569 \[hep-ph\]](https://arxiv.org/abs/1912.02569).

[63] Yann Gouttenoire, Géraldine Servant, and Peera Simakachorn. “BSM with Cosmic Strings: Heavy, up to EeV mass, Unstable Particles”. In: *JCAP* 07 (2020), p. 016. DOI: [10.1088/1475-7516/2020/07/016](https://doi.org/10.1088/1475-7516/2020/07/016). arXiv: [1912.03245 \[hep-ph\]](https://arxiv.org/abs/1912.03245).

[64] Subhasis Maiti and Debaprasad Maity. “The Magnetic Origin of Primordial Black Holes: A Viable Dark Matter Scenario”. In: (Aug. 2025). arXiv: [2508.19217 \[astro-ph.CO\]](https://arxiv.org/abs/2508.19217).

[65] Subhasis Maiti, Debaprasad Maity, and Rohan Srikanth. “Probing reheating phase via non-helical magnetogenesis and secondary gravitational waves”. In: *Phys. Rev. D* 112.6 (2025), p. 063552. DOI: [10.1103/4n86-9nsc](https://doi.org/10.1103/4n86-9nsc). arXiv: [2505.13623 \[astro-ph.CO\]](https://arxiv.org/abs/2505.13623).

[66] Jerome Martin, Christophe Ringeval, and Vincent Vennin. “Observing Inflationary Reheating”. In: *Phys. Rev. Lett.* 114.8 (2015), p. 081303. DOI: [10.1103/PhysRevLett.114.081303](https://doi.org/10.1103/PhysRevLett.114.081303). arXiv: [1410.7958 \[astro-ph.CO\]](https://arxiv.org/abs/1410.7958).

[67] Daniel G. Figueroa and Erwin H. Tanin. “Ability of LIGO and LISA to probe the equation of state of the early Universe”. In: *JCAP* 08 (2019), p. 011. DOI: [10.1088/1475-7516/2019/08/011](https://doi.org/10.1088/1475-7516/2019/08/011). arXiv: [1905.11960 \[astro-ph.CO\]](https://arxiv.org/abs/1905.11960).

[68] Sunny Vagnozzi. “Implications of the NANOGrav results for inflation”. In: *Mon. Not. Roy. Astron. Soc.* 502.1 (2021), pp. L11–L15. DOI: [10.1093/mnrasl/slaa203](https://doi.org/10.1093/mnrasl/slaa203). arXiv: [2009.13432 \[astro-ph.CO\]](https://arxiv.org/abs/2009.13432).

[69] Micol Benetti, Leila Lobato Graef, and Sunny Vagnozzi. “Primordial gravitational waves from NANOGrav: A broken power-law approach”. In: *Phys. Rev. D* 105.4 (2022), p. 043520. DOI: [10.1103/PhysRevD.105.043520](https://doi.org/10.1103/PhysRevD.105.043520). arXiv: [2111.04758 \[astro-ph.CO\]](https://arxiv.org/abs/2111.04758).

[70] Sunny Vagnozzi. “Inflationary interpretation of the stochastic gravitational wave background signal detected by pulsar timing array experiments”. In: *JHEAp* 39 (2023), pp. 81–98. DOI: [10.1016/j.jheap.2023.07.001](https://doi.org/10.1016/j.jheap.2023.07.001). arXiv: [2306.16912 \[astro-ph.CO\]](https://arxiv.org/abs/2306.16912).

[71] Nathalie Deruelle and Viatcheslav F. Mukhanov. “On matching conditions for cosmological perturbations”. In: *Phys. Rev. D* 52 (1995), pp. 5549–5555. DOI: [10.1103/PhysRevD.52.5549](https://doi.org/10.1103/PhysRevD.52.5549). arXiv: [gr-qc/9503050](https://arxiv.org/abs/gr-qc/9503050).

[72] Swagat S. Mishra, Edmund J. Copeland, and Anne M. Green. “Primordial black holes and stochastic inflation beyond slow roll. Part I. Noise matrix elements”. In: *JCAP* 09 (2023), p. 005. DOI: [10.1088/1475-7516/2023/09/005](https://doi.org/10.1088/1475-7516/2023/09/005). arXiv: [2303.17375 \[astro-ph.CO\]](https://arxiv.org/abs/2303.17375).

[73] *NIST Digital Library of Mathematical Functions*. <https://dlmf.nist.gov/>, Release 1.1.12 of 2023-12-15. F. W. J. Olver, A. B. Olde Daalhuis, D. W. Lozier, B. I. Schneider, R. F. Boisvert, C. W. Clark, B. R. Miller, B. V. Saunders, H. S. Cohl, and M. A. McClain, eds. URL: <https://dlmf.nist.gov/>.

[74] Kin-Wang Ng. “Graviton mode function in inflationary cosmology”. In: *Int. J. Mod. Phys. A* 11 (1996), pp. 3175–3193. DOI: [10.1142/S0217751X96001528](https://doi.org/10.1142/S0217751X96001528). arXiv: [gr-qc/9311002](https://arxiv.org/abs/gr-qc/9311002).

[75] Stefan Antusch et al. “Characterizing the postinflationary reheating history: Single daughter field with quadratic-quadratic interaction”. In: *Phys. Rev. D* 105.4 (2022), p. 043532. DOI: [10.1103/PhysRevD.105.043532](https://doi.org/10.1103/PhysRevD.105.043532). arXiv: [2112.11280 \[astro-ph.CO\]](https://arxiv.org/abs/2112.11280).

[76] Kazunori Kohri and Takahiro Terada. “Semianalytic calculation of gravitational wave spectrum nonlinearly induced from primordial curvature perturbations”. In: *Phys. Rev. D* 97.12 (2018), p. 123532. DOI: [10.1103/PhysRevD.97.123532](https://doi.org/10.1103/PhysRevD.97.123532). arXiv: [1804.08577 \[gr-qc\]](https://arxiv.org/abs/1804.08577).

[77] Massimo Giovannini. “Effective energy density of relic gravitons”. In: *Phys. Rev. D* 100.8 (2019), p. 083531. DOI: [10.1103/PhysRevD.100.083531](https://doi.org/10.1103/PhysRevD.100.083531). arXiv: [1908.09679 \[hep-th\]](https://arxiv.org/abs/1908.09679).

[78] Charles R. Harris et al. “Array programming with NumPy”. In: *Nature* 585.7825 (Sept. 2020), pp. 357–362. DOI: [10.1038/s41586-020-2649-2](https://doi.org/10.1038/s41586-020-2649-2). URL: <https://doi.org/10.1038/s41586-020-2649-2>.

[79] Pauli Virtanen et al. “SciPy 1.0: Fundamental Algorithms for Scientific Computing in Python”. In: *Nature Methods* 17 (2020), pp. 261–272. DOI: [10.1038/s41592-019-0686-2](https://doi.org/10.1038/s41592-019-0686-2).

[80] The mpmath development team. *mpmath: a Python library for arbitrary-precision floating-point arithmetic (version 1.3.0)*. <http://mpmath.org/>. 2023.

[81] Fien Apers et al. “String Theory and the First Half of the Universe”. In: (Jan. 2024). arXiv: [2401.04064 \[hep-th\]](https://arxiv.org/abs/2401.04064).

[82] Kishore N. Ananda, Chris Clarkson, and David Wands. “The Cosmological gravitational wave background from primordial density perturbations”. In: *Phys. Rev. D* 75 (2007), p. 123518. DOI: [10.1103/PhysRevD.75.123518](https://doi.org/10.1103/PhysRevD.75.123518). arXiv: [gr-qc/0612013](https://arxiv.org/abs/gr-qc/0612013).

[83] Daniel Baumann et al. “Gravitational Wave Spectrum Induced by Primordial Scalar Perturbations”. In: *Phys. Rev. D* 76 (2007), p. 084019. DOI: [10.1103/PhysRevD.76.084019](https://doi.org/10.1103/PhysRevD.76.084019). arXiv: [hep-th/0703290](https://arxiv.org/abs/hep-th/0703290).

[84] Guillem Domènech. “Scalar Induced Gravitational Waves Review”. In: *Universe* 7.11 (2021), p. 398. DOI: [10.3390/universe7110398](https://doi.org/10.3390/universe7110398). arXiv: [2109.01398 \[gr-qc\]](https://arxiv.org/abs/2109.01398).